Title
RESULTS FROM THE SPEAR MAGNETIC DETECTOR WITH THE LEAD-GLASS-ADDITION

Author
Barbaro-Galtieri, A.

Publication Date
1977-10-01

Proceedings of the 1977 International
Symposium on Lepton and Photon
Interactions at High Energies,
Hamburg, Germany, August 25 - 31, 1977

RESULTS FROM THE SPEAR MAGNETIC DETECTOR WITH THE LEAD-GLASS-ADDITION

A. Barbaro-Galtieri

October 1977

Prepared for the U. S. Department of Energy
under Contract W-7405-ENG-48

DISCLAIMER

RESULTS FROM THE SPEAR MAGNETIC DETECTOR WITH THE LEAD-GLASS-ADDITION*

A. Barbaro-Galtieri
Lawrence Berkeley Laboratory
University of California
Berkeley, California 94720

ABSTRACT

Results from the SP-26 experiment at SPEAR are reported. First we discuss the parameters of the $\psi(3772)$ recently discovered in this experiment. This resonance is just above threshold for D production, therefore we have been able to measure the D masses with high precision. Next we report measurements of D branching fractions into hadronic and semileptonic modes; the hadronic branching fractions are reported here for the first time and include a number of decay modes not observed before. At higher e^+e^- center of mass energies we present some data relevant to charmed baryon production in e^+e^- collisions. Finally, we discuss the data on heavy lepton production obtained in this experiment.

CONTENTS

*Work performed with the support of the U.S. Department of Energy.

I. INTRODUCTION

The SPEAR results presented in this talk come from experiment SP-26 which ran from October 1976 through June 1977. The physicists involved in this experiment[1] overlap only partially with the ones who have built and developed the software for the main detector.[2] Recent results obtained from that experiment, SP-17, can be found in Sadrozinski's talk in these Proceedings.

In order to improve electron and photon detection and resolution, a lead glass system (LGW) has been added to the magnetic detector for part of the solid angle.[3,4] Figure 1 shows a cross section of the modified magnetic detector. Details can be found in Refs. 3 and 4. Briefly, three shower

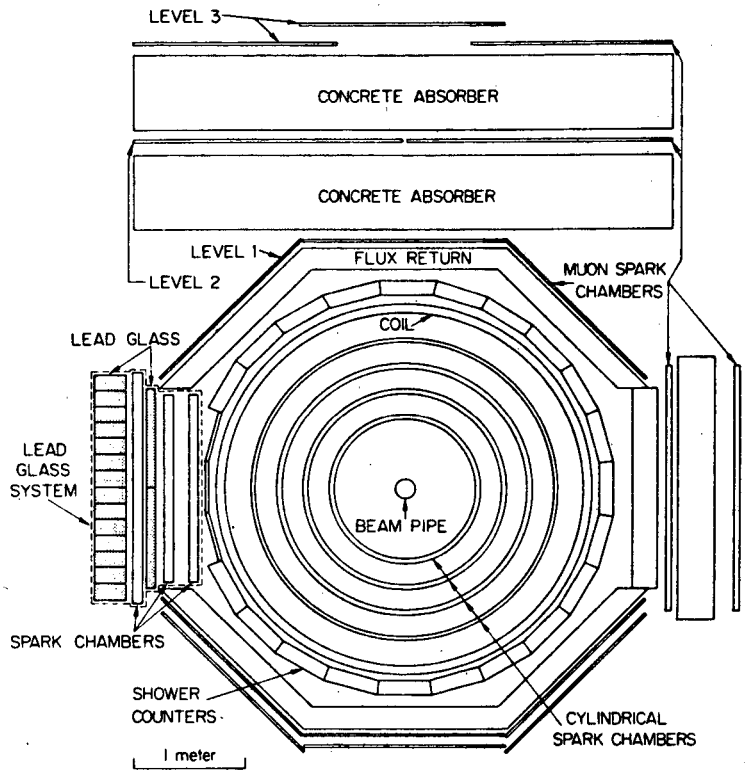

XBL 7711-10393

Fig. 1. Magnetic detector as seen looking along the incident beams. The proportional chambers around the beam pipe and the trigger counters are not shown. The lead glass system (LGW) is shown on the left of the figure. Details on this addition are given in the text, and in Refs. 3 and 4.

counters have been removed and replaced by 1.9-cm thick scintillation counters, and a lead glass system (LGW) has been added. It consists of a 2×26 array of lead glass active converters, 3.3 radiation lengths (X_o) thick; and a 14×19 array of lead glass blocks, 10.5 X_o thick. Two magnetostrictive spark chambers are placed between the coil of the magnet and the active converters and one more chamber is placed between the active converters and the back blocks. Since this system is placed behind the 1 X_o of Al of the magnet coil, its energy resolution is found to be $9\%/\sqrt{E}$, with E given in GeV.

II. THE ψ(3772) STATE

The data on the ψ(3772), ψ", discovered in this experiment, have already been published.[5] Only the main results will be mentioned here. Figure 2 shows the ratio R of the total hadronic cross section to the cross section for μ pair production plotted vs $E_{c.m.}$, center-of-mass energy, in the region

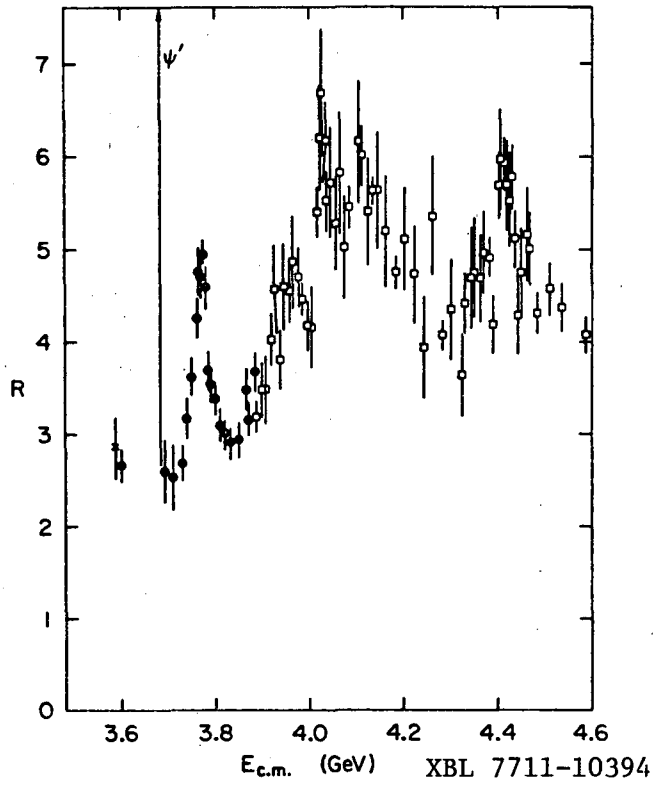

Fig. 2. R versus $E_{c.m.}$. The data points are: ●, this experiment,[5] ×, Augustin et al.,[2] □, Siegrist et al.[6] Radiative corrections have been applied.

3.6 to 4.6 GeV. Data from this experiment are shown in full circles; the other data are published results from SP-17.[2,6] The radiative corrections[7] have already been applied to the data; hence, the height of the ψ" resonance itself is enhanced by a factor[8] of 1.29. Figure 3(a) shows our data before the radiative corrections have been applied; the tail of the ψ(3684) is responsible for the high points below the ψ".

Since this resonance is above $D\bar{D}$ threshold, we have assumed that it decays mostly into $D\bar{D}$, and therefore have used a P-wave Breit-Wigner form, with a momentum dependence calculated for equal contribution of D^o and D^+ mesons. One of the fits obtained with this hypothesis is shown in Fig. 3(b) (here radiative corrections have been applied to the data). The parameters of the ψ" are essentially independent of assumptions on the background form; with systematic errors added, the results are:

$$M = 3772 \pm 6 \text{ MeV}, \qquad \Gamma_e = 0.345 \pm 0.085 \text{ KeV},$$
$$\Gamma = 28 \pm 5 \text{ MeV}, \qquad \Delta R = 2.08 \pm 0.35 .$$

These parameters are shown in Table I along with parameters for other vector mesons decaying into e^+e^-. This value of Γ_e is the revised value, as discussed in Ref. 19.

The ψ" can be identified with the $^3D_1$ state of $c\bar{c}$ predicted at this mass by Eichten et al.,[12] who studied the charmonium spectrum using a linear

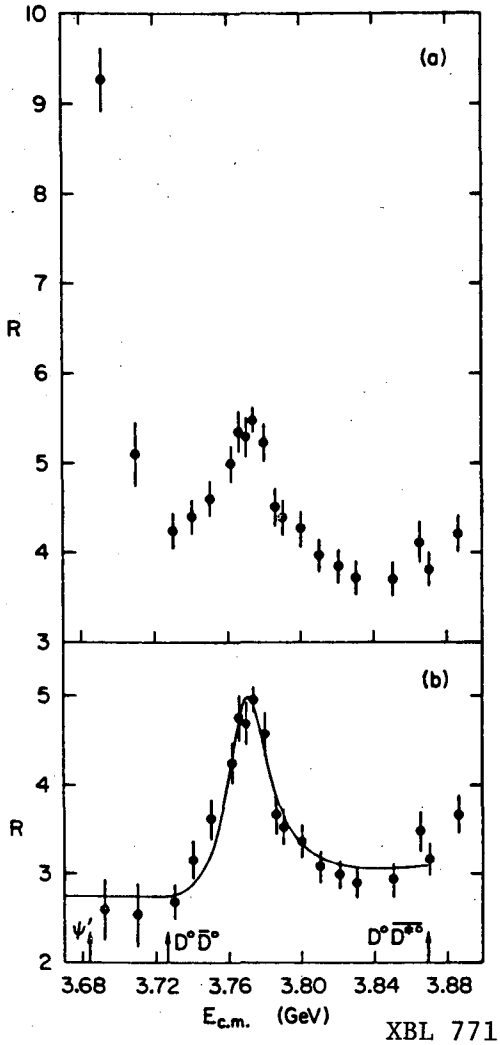

XBL 7711-10395

Fig. 3. R versus $E_{c.m.}$ (a) before and (b) after radiative corrections. The curve is a P-wave Breit-Wigner fitted to the data.

TABLE I. Resonance parameters for vector mesons.[a] Γ is the full width, Γ_{ee} is the partial width to electron pairs, and B_{ee} is the branching fraction to electron pairs.

State	Mass[b] (MeV)	Γ (MeV)	Γ_{ee} (keV)	B_{ee}
$\rho(773)$	773 ± 3	152 ± 3	6.5 ± 0.8	$(4.3 \pm 0.5) \times 10^{-5}$
$\omega(783)$	782.7 ± 0.3	10.0 ± 0.4	0.76 ± 0.17	$(7.6 \pm 1.7) \times 10^{-5}$
$\phi(1020)$	1019.7 ± 0.3	4.1 ± 0.2	1.31 ± 0.10	$(32 \pm 2) \times 10^{-5}$
$\psi(3095)$	3095 ± 4	0.069 ± 0.015	4.8 ± 0.6	$(69 \pm 9) \times 10^{-3}$
$\psi(3684)$	3684 ± 5	0.228 ± 0.056	2.1 ± 0.3	$(9.3 \pm 1.6) \times 10^{-3}$
$\psi(3772)$	3772 ± 6	28 ± 5	0.35 ± 0.09	$(1.2 \pm 0.3) \times 10^{-5}$
$\psi(4414)$	4414 ± 7	33 ± 10	0.44 ± 0.14	$(1.3 \pm 0.3) \times 10^{-5}$

[a] The parameters shown in the Table are taken from Particle Data Group[9] for ρ, ω, ϕ; Boyarski et al.[10] for $\psi(3095)$; Luth et al.[11] for $\psi(3684)$, and Siegrist et al.[6] for $\psi(4414)$.

[b] Errors for ψ states include a 0.13% uncertainty in the absolute energy calibration of SPEAR. The mass difference between the $\psi(3684)$ and $\psi(3772)$ is 88 ± 3 MeV.

form for the confinement potential. In their simple model, the leptonic width, which is proportional to the square of the wave function at the origin, would be $\Gamma_e = 0$ because the $\ell = 2$ wave function vanishes at the origin; however, the ψ'' would be observed because of $^3S_1$-$^3D_1$ mixing with the nearby ψ'. In Ref. 5, we have calculated a mixing angle for these two states based on the model of Ref. 12. However, as pointed out by Jackson,[13] additional terms should be considered into the Γ_e and the mixing angle calculation becomes more complicated than we have assumed. The correct evaluation of this angle will have to wait for more theoretical work.

One final observation is that the total width of the ψ'', $\Gamma = 28$ MeV, is much larger than those of the ψ, $\Gamma = 69$ keV, and of the ψ', $\Gamma = 0.228$ MeV, as expected from the Okuko-Zweig-Izuka rule. In fact, the ψ'' is above $D\bar{D}$ threshold, and it can freely decay into charmed particles. We have measured the cross section times branching ratio $\sigma \cdot B$ for $D^0 \to K^-\pi^+$ across the resonance (Fig. 4); it shows that the D meson is strongly produced at the ψ''. In Section IV we will assume that ψ'' decays entirely into $D\bar{D}$, and in Section V we will see that this assumption is consistent with our branching ratio results.

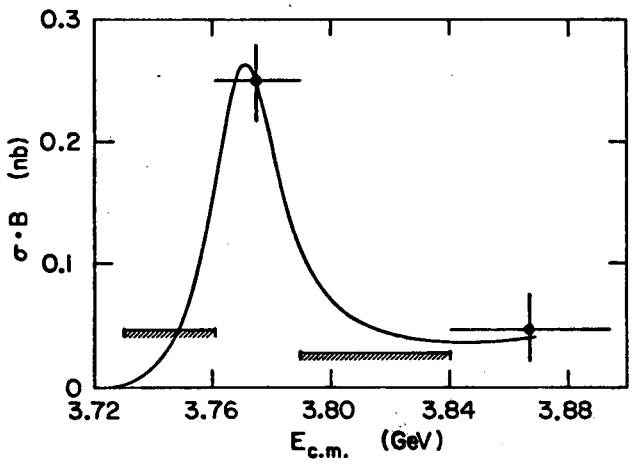

XBL 7711-10396

Fig. 4. Data for $\sigma \cdot B$ versus $E_{c.m.}$ for D^0 and $\bar{D}^0$ decays into $K^{\mp}\pi^{\pm}$. The cross-hatched bars represent 90% CL upper limits. The curve is the same one shown in Fig. 3(b), normalized to the point at 3.774 GeV.

III. PRECISE MASS MEASUREMENTS OF D MESONS

The invariant mass of n particles is calculated by the formula

$$M = \sqrt{(\Sigma E_i)^2 - (\Sigma \vec{p}_i)^2} \qquad (1)$$

where the Σ is over the n particles. At the ψ'' we can measure the masses of the D mesons with better precision than previously done.[14] In fact, since the ψ'' is so close to threshold for $D\bar{D}$ production, we can use the following facts to improve the mass resolution:

(a) No other particles can be produced besides the D and $\bar{D}$. We can then assume that the D energy, $\sum_{i=1}^{n}(E_i)$, is the same as the beam energy, E_b, which is much better determined than the energy obtained by the momentum measurements of the tracking system of the magnetic detector. The rms error of E_b is 1 MeV[15] and its central value can be monitored with high precision.[16]

(b) The momenta of the secondary particles are low. In fact, $p_D \sim 300$ MeV/c and the effect of the uncertainty in p on the mass error is small.

The overall resolution is of about 3 MeV, and the final error is dominated by systematic errors rather than statistical errors.[16]

For each event we identify charged kaons by time-of-flight measurements,[17] and neutral kaons by calculating the $\pi^+\pi^-$ invariant mass and then applying appropriate cuts to reduce the background.[18] We then calculate the energy for all K and $(n-1)\pi$ combinations possible in the event, select those for which $\sum_{i=1}^{n} E_i$ agrees with E_b within 50 MeV and calculate the invariant mass for these combinations using E_b instead of the measured energy.[19] The invariant mass plots for the most copious decay modes of the D^+ and D^o are shown in Fig. 5. The results for the masses are shown in Table II.

TABLE II. Masses, mass differences, and Q values for the D meson system.[19] The quantities in parentheses are taken from Refs. 14 and 20 and are used in the calculation of quantities involving D^*'s. All units are MeV. See text for a discussion of errors.

Mass (MeV)		Mass Difference (MeV)		Q Values (MeV)	
D^o	1863.3 ± 0.9	$D^+ - D^o$	5.0 ± 0.8	$D^{*o} \to D^o\pi^o$	7.7 ± 1.7
D^+	1868.3 ± 0.9	$D^{*+} - D^{*o}$	2.6 ± 1.8	$D^{*o} \to D^+\pi^-$	-1.9 ± 1.7
D^{*o}	(2006.0 ± 1.5)	$(D^+-D^o)-(D^{*+}-D^{*o})$	2.4 ± 2.4	$D^{*+} \to D^o\pi^+$	(5.7 ± 0.5)
D^{*+}	2008.6 ± 1.0			$D^{*+} \to D^+\pi^o$	5.3 ± 0.9

The mass difference is better determined than the individual masses because some of the systematic errors cancel out in the mass difference.[16] The value $M_o - M_+ = 5.0 \pm 0.8$ MeV agrees with theoretical expectations.[21] We can now use the published values[14,20] of the D^{*o} mass and the Q for $D^{*+} \to D^o\pi^+$ and improve on the D^{*+} mass value and the other Q values for D^* decays. These results are also shown in Table II.

IV. MEASUREMENT OF D BRANCHING FRACTIONS

A. Method

For the first time we can calculate, with relatively few assumptions, branching fractions for D decays.[19] If N_i is the number of D events found in channel i, we can write

$$N_i = 2\sigma(e^+e^- \to D\bar{D})\, B_i A_i L \qquad (2)$$

where B_i and A_i are the branching fraction and the acceptance for that D

decay mode, L is the total integrated luminosity of the sample analyzed, and the factor 2 indicates that either D can decay into that mode.

In previous studies of the D meson properties,[22] it has been difficult to evaluate σ for D production, therefore only $\sigma \cdot B$ values were measured. At the ψ'' we can calculate σ for D^+ and D^o production with the following assumptions:

(a) The ψ'' decays entirely into $D\bar{D}$. As discussed in Section II, this is a reasonable assumption.

(b) The ψ'' is in a definite Isospin State (0 or 1). In this case, we can expect that D^+ and D^o are produced equally except for barrier factors. For P-wave we get for the ratio of the rates

$$\frac{\Gamma(D^o)}{\Gamma(D^+)} = \frac{p_o^3[1+(rp_+)^2]}{p_+^3[1+(rp_o)^2]} \qquad (3)$$

where p_+, p_o are the momenta of the D^+ and D^o respectively, and r is the radius of interaction.

It turns out that the ratio (3) is not too sensitive to the value of r; in fact, the fraction of $D^o\bar{D}^o$ varies between 0.59 and 0.53 for r between 0 and infinity. We take this fraction to be 0.56 ± 0.03. This fraction is energy dependent; however, the data sample we used for branching fraction determination is confined to $3.76 < E_{cm} < 3.79$ GeV, with about 70% of the data at the fixed energy E = 3.774 GeV, where we have calculated the fraction quoted above.

With the two previous assumptions and the data of Ref. 5 we get

$$2\sigma(e^+e^- \to D^o\bar{D}^o) = 11.5 \pm 2.5 \text{ nb}\ , \quad 2\sigma(e^+e^- \to D^+D^-) = 9.2 \pm 2.0 \text{ nb} \qquad (4)$$

B. Hadronic Decays with a K and Charged Pions

The mass plots for the D decay modes with a K meson and all charged pions in the final state are shown in Fig. 5. The sample used has an integrated luminosity $L = 1.21\ pb^{-1}$. The acceptance of the apparatus A_i includes geometrical acceptance as well as efficiency of the apparatus for triggering (two charged particles are required), track reconstruction, time-of-flight identification of kaons, etc. The acceptance has been calculated by a Monte Carlo program; more details can be found in Ref. 19. The number of events in each channel and the calculated branching fractions are given in Table III; the errors in B_i include systematic uncertainties. Figure 5 and Table III show that we have a good signal for the $D^+ \to \bar{K}^o\pi^+$ decay mode. This mode would be suppressed if the $\Delta I = \frac{1}{2}$ rule observed in SU(3) is extended to SU(4). Some authors[23] have argued that if the octet enhancement phenomena that has been introduced to explain the $\Delta I = \frac{1}{2}$ rule is extended to SU(4), one expects 20-plet enhancement and therefore suppression of modes which belong to the $\underline{84}$ representation of SU(4), like the $D^+ \to \bar{K}^o\pi^+$. For comparisons with models we give

$$\frac{\Gamma(D^+ \to \bar{K}^o\pi^+)}{\Gamma(D^o \to K^-\pi^+)} = 0.70 \pm 0.23 \qquad (5)$$

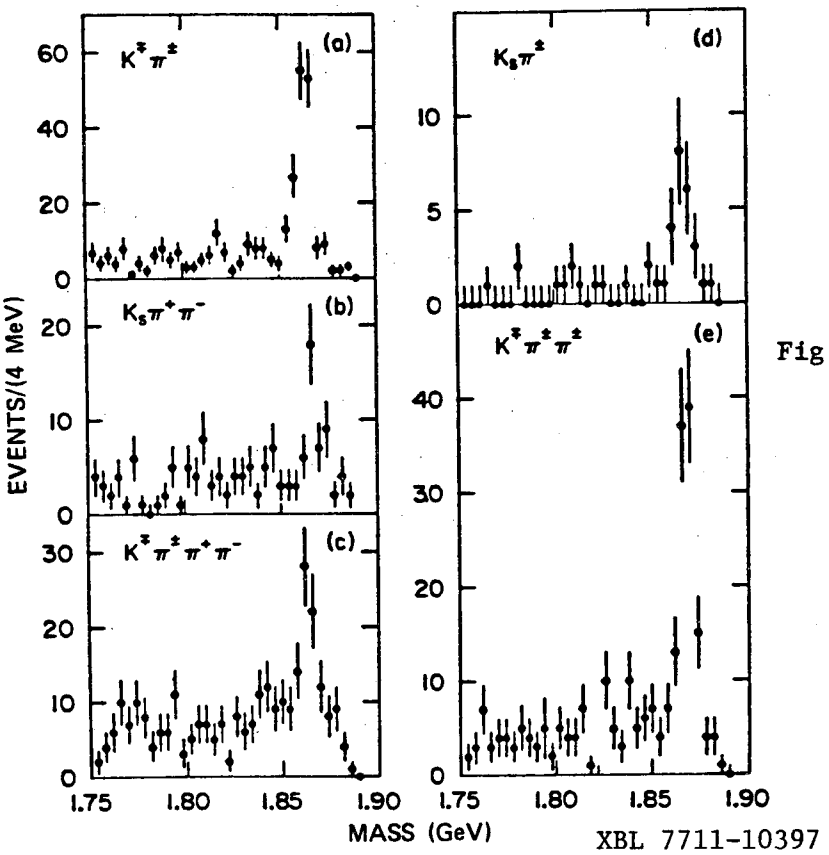

Fig. 5. Invariant mass spectra for various D^o (on the left) and D^+ (on the right) decay modes. Note that the distributions are plotted in 4 MeV bins.

TABLE III. Number of combinations and branching fractions, B_i, for various D decay modes.[19]

Mode	Number Combination	B_i (%)
$K^{\mp}\pi^{\pm}$	130 ± 13	2.2 ± 0.6
$\bar{K}^o\pi^+\pi^-$ + c.c.	28 ± 7	4.0 ± 1.3
$K^{\mp}\pi^{\pm}\pi^+\pi^-$	44 ± 10	3.2 ± 1.1
. . . . .	. . . . .	. . . . .
$\bar{K}^o\pi^+$ + c.c.	17 ± 5	1.5 ± 0.6
$K^{\mp}\pi^{\pm}\pi^{\pm}$	85 ± 11	3.9 ± 1.0

which has a smaller error than the ratio of the branching fractions of Table III, since some systematic errors cancel out.

C. The Decay $D^o \to K^-\pi^+\pi^o$

Using the lead glass wall information we have found some events[24] of the type

$$D^o \to K^-\pi^+\pi^o \quad \text{and} \quad \text{c.c.} \tag{6}$$

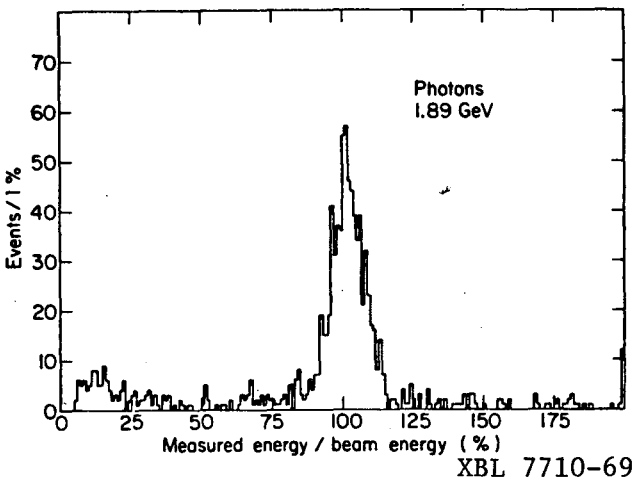

XBL 7710-6928

Fig. 6. Ratio of the measured energy over the beam energy for γ rays in the lead glass wall for the reaction $e^+e^- \to \gamma\gamma$. These data are at the $\psi(3772)$; the energy resolution is $\sigma_\gamma/E_\gamma = 5.8\%$.

Figure 6 shows the energy distribution for γ rays measured in the lead glass wall (LGW) for events for which a second γ ray is detected in the magnetic detector shower counters opposite the LGW. These events are of the type $e^+e^- \to \gamma\gamma$ and the beam energy is at the $\psi(3772)$. The energy resolution for γ's of this energy is found to be 5.8%, and we expect it to vary with energy according to the formula $\sigma_\gamma/E_\gamma = 8\%/\sqrt{E_\gamma}$, E_γ in GeV. There is some background because no kinematical constraints have been applied.

To find π^0's from reaction (6) we calculate the invariant mass $M_{\gamma\gamma}$ for those events for which we have $N_\gamma \geq 2$ in the lead glass wall and at least two charged particles in the detector. This distribution is shown in Fig. 7, where only photons with $E_\gamma > 150$ MeV were used. The mass resolution is

$$\frac{\sigma_{\pi^0}}{M_{\pi^0}} = 18\% \ .$$

We expect this resolution to improve in the future, since we are still working on calibration of low energy γ rays and other aspects of γ energy measurements.

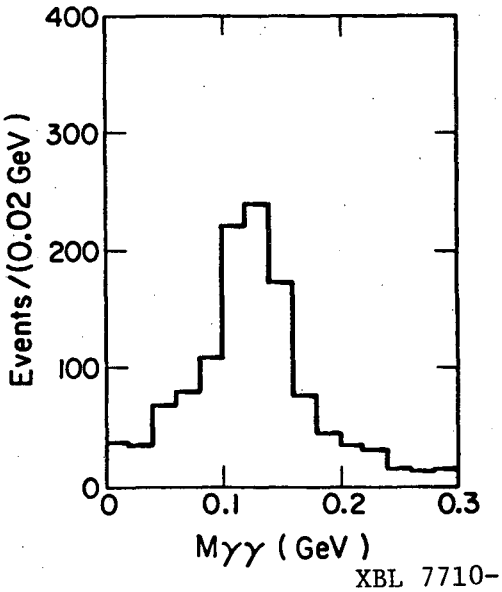

XBL 7710-6931

Fig. 7. The two γ invariant mass distribution, $M_{\gamma\gamma}$, for events with at least two γ rays in the lead glass wall. Only combinations with each photons having $E_\gamma > 150$ MeV are shown.

The lead glass wall covers only 6% of the solid angle (10% of the solid angle covered by the magnetic detector), therefore the acceptance for reaction (6) is small. This acceptance has been calculated by Monte Carlo simulation and includes all the efficiencies of the apparatus as discussed in Section IV.B. Figure 8 shows the invariant mass distribution of the $K\pi\pi^o$ system calculated using formula (1) with

$$\sum_{i=1}^{3} (E_i) = E_b$$

as for the other hadronic decays. There are nine events near the D^o mass with a mean value of 1861 MeV, consistent with the D^o mass we have measured in other channels (Section III). The background is estimated by counting the events in the 1.70 to 1.85 GeV region, and it is found to be 1.7 events. The 7.3 ± 3.0 events in excess give a branching fraction[24] for reaction (6)

$$B(D^o \to K^-\pi^+\pi^o) = (12 \pm 6)\%$$

where systematic errors have been included.

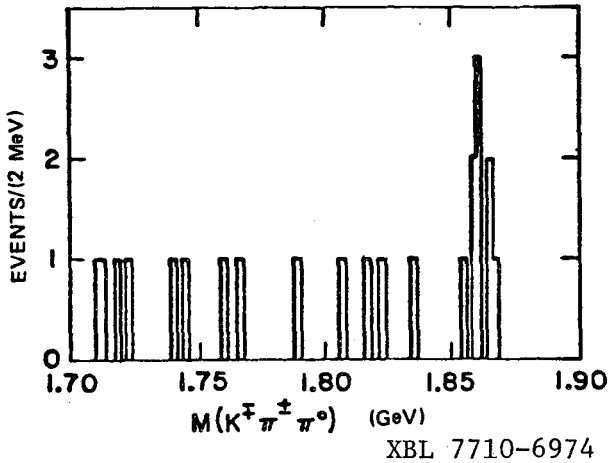

XBL 7710-6974

Fig. 8. The $K^{\mp}\pi^{\pm}\pi^o$ invariant mass for events with a π^o in the LGW, at the $\psi(3772)$. A cluster of events appears at the D^o mass, giving evidence for $D^o \to K^-\pi^+\pi^o$ and the charge conjugate reaction.

D. Semileptonic Decays of D Mesons into Electrons

We have measured the branching fraction[25] of the decay mode $D \to eX$ (assuming $D \to K e \nu_e$ or $K^* e \nu_e$) at the ψ'' using the assumptions of Section IV.A. We also have preliminary results on an estimate of this branching fraction at other e^+e^- energies.[26]

The electrons are identified in the lead glass wall. Figure 9 shows the energy resolution of the lead glass system for electrons of the reaction $e^+e^- \to e^+e^-$ at the ψ''. The e-π separation is achieved by measuring separately the energy, E_{AC}, deposited in the first 3.3 X_o of the lead glass and the energy, E_{BB}, deposited in the remaining 10.5 X_o, since the electromagnetic shower of an electron and the hadronic shower of a π have different behavior at different depths into a given material. For electrons we require typically (the actual criteria change slightly with momentum) $E_{AC} \geq 150$ MeV to eliminate noninteracting particles, $E_{BB} > 0.1\,E$ and $(E_{AC} + E_{BB}) \geq 0.65\,E$, where E is the energy of the electron as measured in the magnetic detector. More details can be found in Ref. 26. We have used data at the $\psi(3095)$ to determine the background due to hadron misidentification, photon conversions and Dalitz decays of π^o and η's which result in a pair of electrons of which only one is

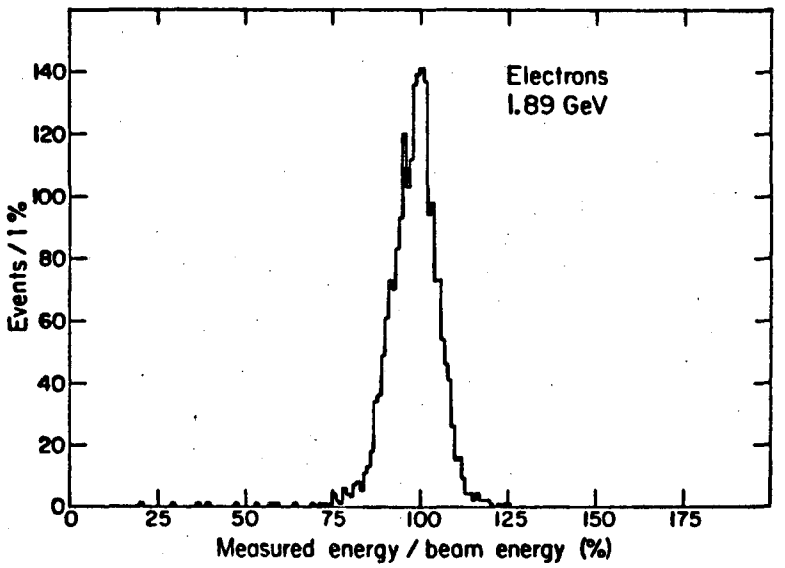

XBL 7710-6927

Fig. 9. Ratio of the energy measured in the lead glass wall over the beam energy for electrons of the reaction $e^+e^- \to e^+e^-$ at the $\psi(3772)$. The energy resolution is $\sigma_e/E_e \approx 6.7\%$.

detected in the apparatus. The background per particle in the LGW varies between 1.4% at 300 MeV/c and 0.4% at $p \geq 1$ GeV/c; its average over the hadron momentum spectrum is 1.1%. At higher energies to this value we have to add the additional contribution from γ conversions and Dalitz decays due to increase in π^o and η productions. The increase of this contribution from the value at the ψ is, at most, 0.4% at $p = 300$ MeV/c and $E_{beam} \geq 3.2$ GeV. With our selection criteria, the average detection efficiency for electrons is 75%, and it has been determined by using the QED processes $e^+e^- \to e^+e^-$, $e^+e^-\gamma$, and $e^+e^-e^+e^-$.

Events of the type

$$e^+e^- \to e^\pm + \geq 2 \text{ charged prongs} + n\gamma \quad (n \geq 0) \qquad (7)$$

have been used to determine the semileptonic branching fraction of the D's. Only multiprong events are used because heavy lepton production and decay is also expected to produce electrons in the final state. However, about 85% of the reaction $e^+e^- \to \tau^+\tau^-$ with one electron in the final state will have only one additional prong. (See Section VIII and Ref. 3.)

At the ψ'' we find a total of 61 events which pass our criteria for reaction (7) in a sample corresponding to 1.34 pb^{-1} integrated luminosity. After background subtraction and efficiency correction this corresponds to 53 ± 15 events.[25] The momentum spectrum for $p \geq 300$ MeV/c is shown in Fig. 10. The curves represent the expected spectra[27] for D meson production $e^+e^- \to \psi(3772) \to D\bar{D}$ with subsequent decay of the D into $\pi e \nu_e$, $K e \nu_e$ and $K^* e \nu_e$ (V-A coupling has been used). The data are somewhat inconsistent with the Cabibbo suppressed mode $\pi e \nu_e$ (confidence level CL = 3%) but are consistent with both the $D \to K e \nu_e$ (CL = 33%) and $D \to K^* e \nu$(V-A) (CL = 13%) decay modes.[28] The best fit to a combination of the last two decay modes gives the contribution of the $D \to Ke\nu$ decay to be (57 ± 30)% of the total.

The acceptance for the K or K^* decay modes has been evaluated by Monte Carlo calculations. This is somewhat dependent upon the electron spectrum of the semileptonic decay and the average charge multiplicity of the hadronic decay of the other D, $\langle n_{ch} \rangle$. We have used $\langle n_{ch} \rangle = 2.3$ as experimentally

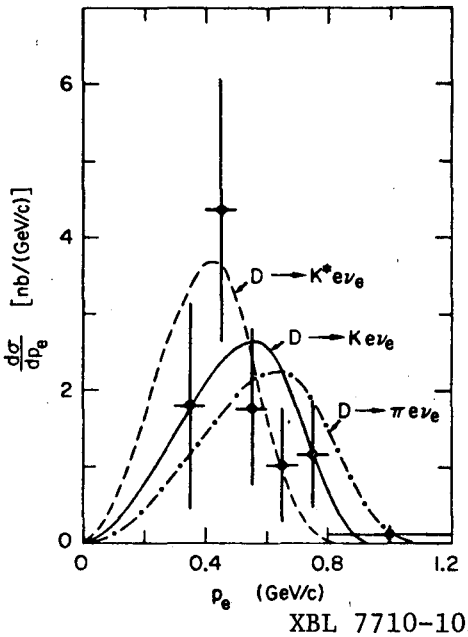

Fig. 10. The electron momentum spectrum for events of the type $e^+e^- \to e^\pm + X$ ($\geq$ 2 charged prongs) at the $\psi(3772)$. The curves are expected spectra calculated from those given by Ali and Yang.[27]

determined (see Section V and Ref. 21). Assuming that $D \to K e \nu_e$ and $D \to K^* e \nu_e$ contribute equally, we get

$$B(D \to eX) = (7.2 \pm 2.6)\%$$

We also have data at energies higher than the ψ''. The electron momentum spectra are shown in Fig. 11. The curves shown have been calculated from the center-of-mass spectra given by Ali and Yang[27] assuming the reaction mechanism $e^+e^- \to D^*\bar{D}^*$ at 4.16 GeV and the 4.4 - 5.7 GeV region, and $e^+e^- \to D^*\bar{D}^*\pi\pi$ at the higher energies.

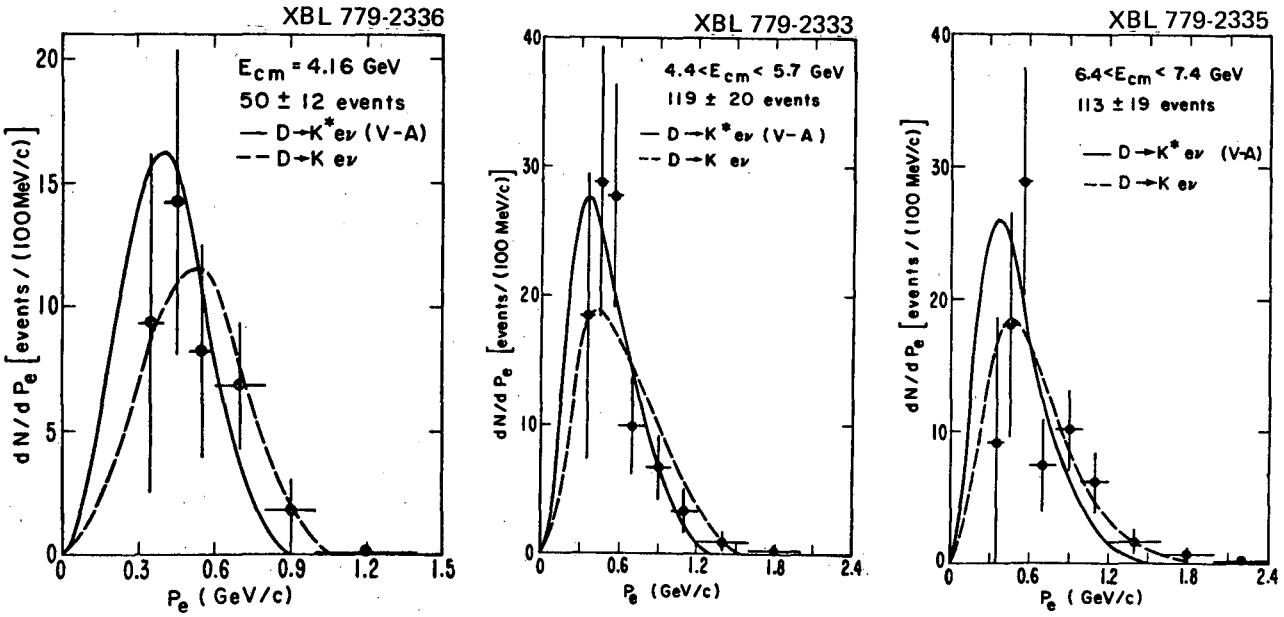

Fig. 11. Preliminary electron momentum spectra for $P_e > 300$ MeV/c in three different $E_{c.m.}$ regions. The curves are normalized to the events seen for $P_e > 300$ MeV/c and are derived from the spectra given in Ref. 27.

As previously pointed out, it is difficult to evaluate σ_D to use in relation (2) at these energies. It is also difficult to determine whether the electrons are decay products of D mesons, F mesons, or charmed baryons. We can estimate a value for the $D \to eK\nu$ or $eK^*\nu$ also from these data assuming: 1) all the electrons after background subtraction come from D mesons (this assumption is needed to calculate the acceptance of the apparatus), and 2) $R_D = R_{charm} = R - R_\tau - R_{old}$, where R_{old} is the constant value of R below charm threshold. Since charmed baryon production is very small (see Section VII) and F production is not known, these may turn out to be not too unreasonable assumptions. We use $R_{old} = 2.6$; R_τ is calculated with $M_\tau = 1.9$ GeV and R is from SPEAR data.[29] Preliminary results of this analysis[26] are given in Table IV. The data at the $\psi(3772)$ are also shown in the table for completeness; as discussed earlier, this branching fraction determination is relatively assumption free. In calculating R_e, we have removed the contribution from heavy lepton decay into multiprong electrons; it varies from 0 to 18 ± 5 events at the highest energy. Figure 12(a) shows a plot of R_e as a function of $E_{c.m.}$. Notice that below and above ψ'' the electron production is consistent with zero, which shows that the e signal is associated with D production. Figure 12(b) shows the variation of B_e with energy.

TABLE IV. Branching fractions for the semileptonic decay of the D meson into electrons. See discussion in the text for the assumption used and for explanation of symbols.

$E_{c.m.}$ (GeV)	L (pb^{-1})	Corrected events	R_e ($p_e > 300$ MeV/c)	R_{charm}	$B_{D \to e}$ (%)
$\psi(3772)$	1.3	53 ± 15	0.17 ± 0.04	1.7 ± 0.3	7.2 ± 2.6
4.1 - 4.2	1.01	50 ± 12	0.26 ± 0.08	2.1 ± 0.5	7.7 ± 3.0
4.4 - 5.7	3.46	119 ± 20	0.23 ± 0.06	1.9 ± 0.5	7.4 ± 2.8
6.4 - 7.4	5.37	113 ± 19	0.26 ± 0.06	1.9 ± 0.4	8.7 ± 3.2

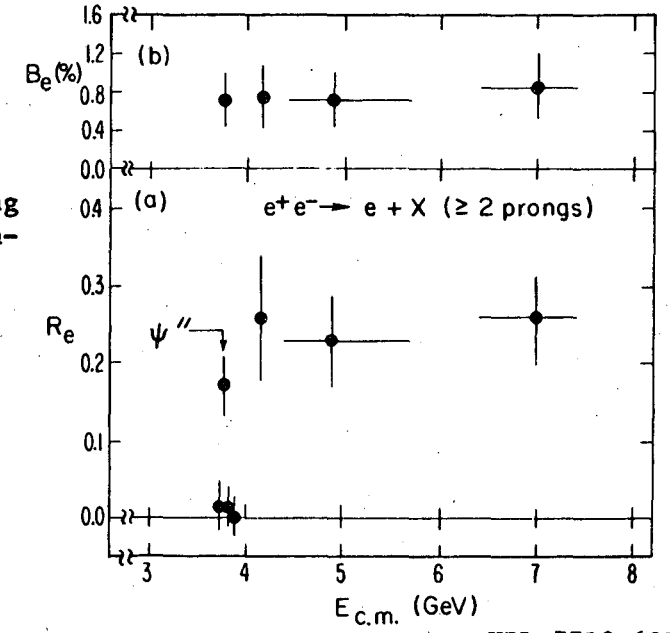

XBL 7710-6973

Fig. 12. (a) The value of $R_e = \sigma_e/\sigma_{\mu\mu}$ versus $E_{c.m.}$ for electrons with $p > 300$ MeV/c in multiprong events. (b) The D branching ratios as a function of $E_{c.m.}$, see text for assumptions made. Results above 4 GeV are preliminary.
XBL 7710-6973

V. TAGGED EVENTS

At the $\psi(3772)$ every D produced should be accompanied by a $\bar{D}$ for charm conservation. We can use this fact to "tag" D events; that is, if we have detected a D or $\bar{D}$ in an event we know that what is recoiling against it must be a $\bar{D}$ or a D. As noted earlier, there is not enough energy at the ψ'' to produce another pion or D^*. In our data we have "tagged"

$$130\ D^0 \quad \text{or} \quad \bar{D}^0 \to K^{\mp}\pi^{\pm}$$

$$85\ \ D^{\pm} \to K^{\mp}\pi^{\pm}\pi^{\pm}$$

Preliminary results from this analysis will be presented here (see also Ref. 21).

A. Absolute Branching Fraction Determinations

The branching fractions B_i can now be measured independently of any assumptions on the individual cross sections, using the expression

$$B_i' = \frac{N_i}{\epsilon_i N_D}$$

where N_i is the observed number of events of the i^{th} decay mode, ϵ_i is the corresponding detection efficiency, and N_D is the number of tagged events.

We have some events for which all the particles in the final state have been observed. We can use these events to calculate branching fractions to compare with the values obtained in Section IV.B, calculated assuming: 1) the ψ'' decays only into $D\bar{D}$; 2) $D\bar{D}$ has definite isospin (0 or 1). Table V shows the results for those modes with at least two events. Among the other events, there are examples of

$$D^0 \to K^0_S\pi^+\pi^-\pi^+\pi^-$$

$$D^+ \to K^0_S\pi^+\pi^-\pi^+$$

Table V shows that for the three cases in which we could measure the branching fraction with this method, the results are in good agreement with those

TABLE V. Comparison of D branching fractions as calculated with the tagged events (B_i') and with the method of Section IV.B, (B_i).

Tagging D^a	Mode^a	N_i	B_i' (%)	B_i (%)
$D^0 \to K^-\pi^+$	$K^+\pi^-$	2	4.5 ± 2.2	2.2 ± 0.6
$\to K^-\pi^+$	$\bar{K}^0\pi^+\pi^-$	2	5.5 ± 3.0	4.0 ± 1.3
$D^+ \to K^-\pi^+\pi^+$	$K^+\pi^-\pi^-$	2	3.4 ± 2.4	3.9 ± 1.1

^{a}Each event has either the decay modes indicated here or their charge conjugates.

obtained earlier, proving that the above assumptions are reasonable. This analysis is continuing, and efforts are being made to fit all the events where one single particle is missing.

B. Charge Multiplicity Determination

We can use the "tagged" D events to determine the average charged multiplicity of D decays. Since the solid angle of the detector is not 4π, we have to calculate the efficiencies for detecting a given number of charged particles and then, given the observed multiplicity distribution, we can use these efficiencies to obtain the true n_{ch} distributions of the D decays. The unfolding matrix has been determined by Monte Carlo calculations. Figure 13 shows the observed distributions and the preliminary unfolded n_{ch} distributions for D^o and D^+ decays. The average values are

$$\langle n_{ch} \rangle = 2.3 \pm 0.2 \quad \text{for } D^o \tag{9a}$$

$$\langle n_{ch} \rangle = 2.3 \pm 0.3 \quad \text{for } D^+ \tag{9b}$$

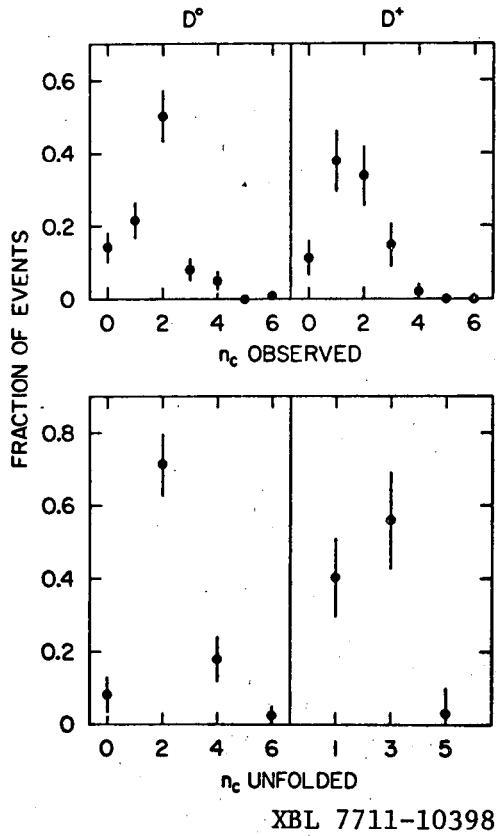

Fig. 13. Distribution of number of charged prongs in "tagged" D decays. The observed multiplicities are shown in the two upper plots, the corrected (unfolded) distributions are shown in the lower plots.[21]

VI. COMPARISON WITH THE STATISTICAL MODEL

Table VI is a summary of all the D^o and D^+ decay modes we have observed and their branching fractions. Assuming μ-e universality, and therefore doubling the D semileptonic decays into electrons, we have measured a total of $(35.8 \pm 7.3)\%$ of the D^o and $(19.8 \pm 3.9)\%$ of the D^+ decay modes. What are the other decay modes? Continuing studies of the tagged D events will undoubtedly improve our knowledge, although the statistics are not large enough to answer all the questions.

TABLE VI. Summary of D decay modes and branching fractions measured in this experiment.[19,24,25]

Mode	B (%)
$D^o \to K^-\pi^+$	2.2 ± 0.6
$\bar{K}^o\pi^+\pi^-$	4.0 ± 1.3
$K^-\pi^+\pi^-\pi^+$	3.2 ± 1.1
$K^-\pi^+\pi^o$	12 ± 6
$\bar{K}^o\pi^+\pi^-\pi^+\pi^-$	seen
eX^a	7.2 ± 2.6
$D^+ \to \bar{K}^o\pi^+$	1.5 ± 0.6
$K^-\pi^+\pi^+$	3.9 ± 1.0
$\bar{K}^o\pi^+\pi^-\pi^+$	seen
eX^a	7.2 ± 2.6

[a] These branching ratios are calculated assuming $D \to Ke\nu$ or $K^*e\nu$, and that $B(D^o \to e) = B(D^+ \to e)$.

We will now compare our results with the statistical model of Quigg and Rosner.[30] These authors have recently calculated the branching ratios of charmed mesons into various hadronic modes using two different models for hadron multiplicity distributions: a) a statistical model, and b) a constant matrix element (c.m.e.) model. Their choice of parameters for the statistical model gives $\langle n_{ch} \rangle = 3.0$ for D^o and $\langle n_{ch} \rangle = 3.1$ for D^+ hadronic decays. These values are larger than our experimental values given in Eq. (9). Their c.m.e. model gives smaller average values for charged multiplicities, that is, $\langle n_{ch} \rangle = 2.4$ for D^o and $\langle n_{ch} \rangle = 2.5$ for D^+ decays, however, the individual branching ratios [for example, $B(D^o \to \bar{K}^o\pi^+\pi^-) = 14.5\%$, $B(D^o \to K^-\pi^+) = 4.7\%$ and $B(D^+ \to K^-\pi^+\pi^+) = 12.8\%$] are considerably different from our experimental values of Table VI.

Figures 14 and 15, taken from Quigg and Rosner (QR), show the expected branching ratios to all the K+pions decay modes for the statistical model with our values shown for comparison. The following comments are relevent for the comparison:

1) For the D^- we have normalized our hadronic branching fractions to 75% instead of 100%. In fact, the QR plots show percent of hadronic

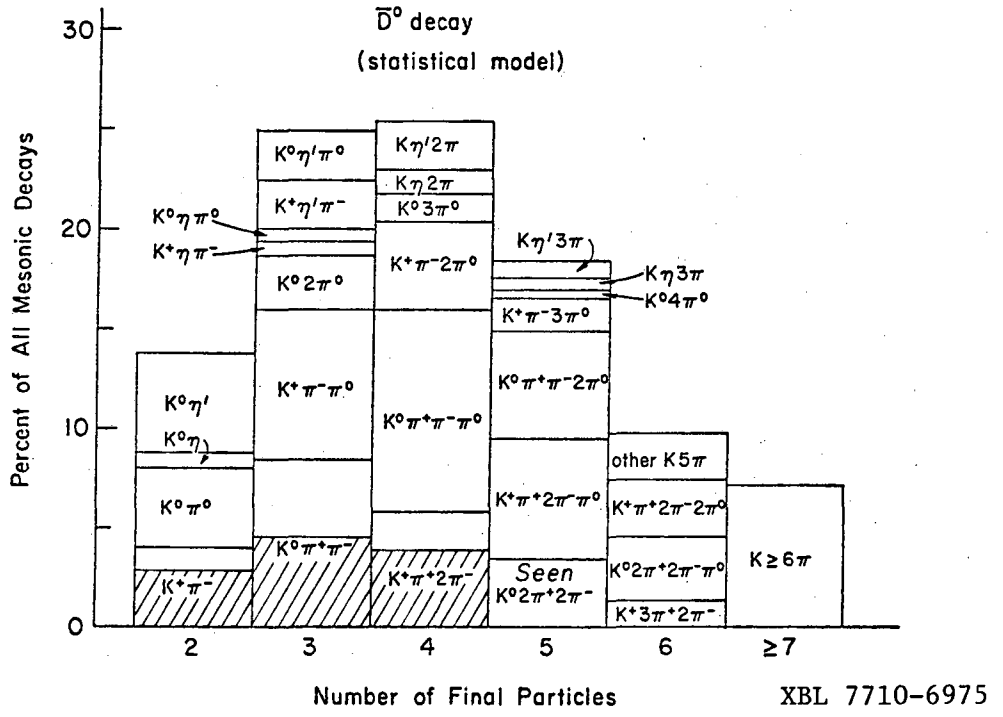

Fig. 14. Prediction of the statistical model of Quigg and Rosner[30] for $\bar{D}^0$ decay into all mesonic decay modes. Our results, normalized to 85% (see text), are shown by the cross-hatched areas. For the $D^0 \to K^-\pi^+\pi^0$ decay mode we have a value $B' = (14 \pm 7)\%$ which is larger than the predicted value, but since the error is very large, we have cross-hatched only the expected area (7.7%).

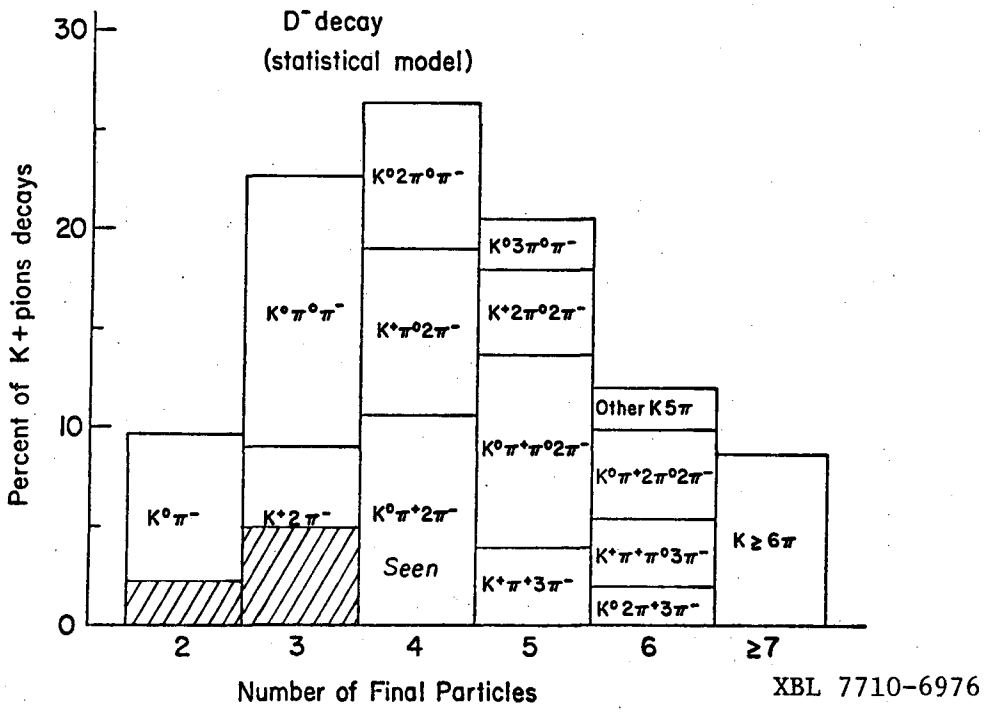

Fig. 15. Prediction of the statistical model of Quigg and Rosner[30] for the D^- decays into K+pions. Our results, normalized to 75% (see text) are shown by the cross-hatched areas.

modes into K + pions, the contribution of the other hadronic modes is expected to be of the order of 10 to 15%. So we calculate

$$B_{Kn\pi} = 1.0 - 0.12\ (1.0 - B_\ell) - B_\ell = 0.75$$

where we have taken 12% to be the other hadronic modes and $B_\ell = 15\%$ is the branching fraction for all the semileptonic modes (see Table VI).

2) For the D^o the decay modes into η and η' are included in Fig. 14, so we normalize to 85% ($B_{hadronic} = 1.0 - B_\ell = 0.85$).

3) The statistical model does not include any considerations of dynamics, so the 20-plet enhancement discussed in Section IV.B does not enter the branching ratio predictions. The $D^+ \to \bar{K}^o\pi^+$ decay mode is calculated using a statistical isospin model, therefore the possible suppression of this mode does not appear in Fig. 15.

In conclusion, the statistical model seems to be in disagreement with the present results on branching fractions. However, many decay modes are still to be measured and certainly we will know more when our analysis of the tagged events is completed.

VII. INCLUSIVE PRODUCTION OF $\bar{p}$, Λ and $\bar{\Lambda}$

We have collected a total of 3.1 pb^{-1} integrated luminosity between 4.5 and 5.7 GeV with the aim of studying charmed baryon production. We have looked at various channels like $\Lambda\pi$, $\Lambda\pi\pi\pi$, but we have found no significant signal for charmed baryons. However, the inclusive cross sections for production of $\bar{p}$, Λ and $\bar{\Lambda}$ show a rise when the energy changes across the thresholds for charmed baryon production. If these particles were produced, such a rise would be expected since $\bar{p}$, Λ and $\bar{\Lambda}$ should be part of their decay products.

Figure 16(a) shows the value of R for Λ and $\bar{\Lambda}$ production in the 3.77 to 7.4 GeV region, measured by this experiment.[31] As discussed in Ref. 31, the

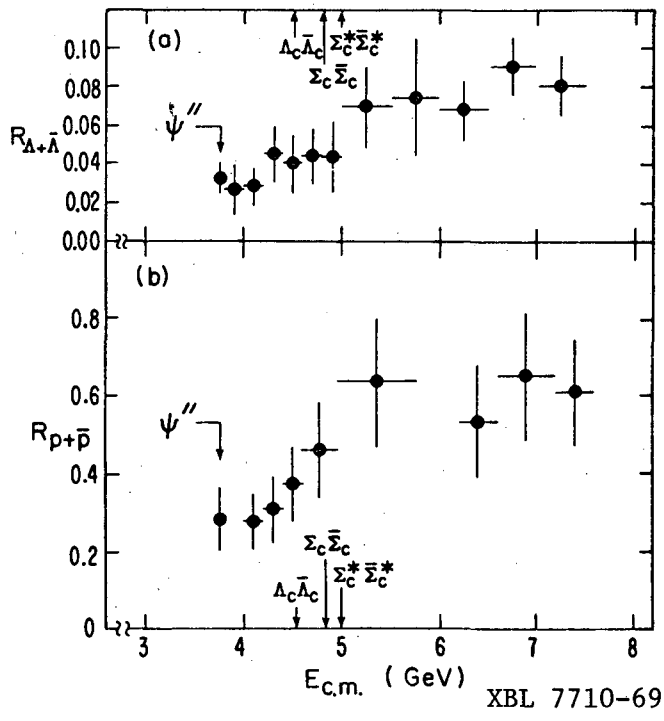

Fig. 16. (a) The measured values of R for Λ and $\bar{\Lambda}$ production versus $E_{c.m.}$ (b) Twice the measured value of R for $\bar{p}$ production versus $E_{c.m.}$ The arrows point to the thresholds for charmed baryon pair production calculated with the assumptions explained in the text.

Λ and $\bar{\Lambda}$ are detected as peaks in the $p\pi^-$ and $\bar{p}\pi^+$ invariant mass plots. The plots are obtained using p and $\bar{p}$ identified by time of flight (TOF) and other requirements necessary to reduce the background. Monte Carlo calculations are used to determine the efficiencies; they vary between 12% at 3.77 GeV and 18% at 7.4 GeV.

Figure 16(b) shows the value of $R_{p+\bar{p}}$ versus $E_{c.m.}$ as obtained in the data of SP-26.[31] Here we have really measured $R_{\bar{p}}$ and then multiplied it by two, assuming that $\bar{p}$ and p are equally produced; this is done because the p have a larger background due to e-p interactions in the residual gas of the beam pipe. The $\bar{p}$ are identified unambiguously by TOF up to 1 GeV/c; between 1 and 2 GeV/c a "weight" method is applied which requires π, K and p separation on a statistical basis, as described in Ref. 31. Very few $\bar{p}$ are produced with $p > 2$ GeV/c and we evaluate this contribution to be < 9% of the cross section, $\sigma_{\bar{p}}$, at all energies.

Figure 16 shows the thresholds for charmed baryon pair production calculated from the mass formula of De Rujula, Georgi, Glashow[32] and using the values of the masses observed in the event of Cazzoli et al.[33] and the photoproduction data.[33]

If we assume that the increase of $p+\bar{p}$ and $\Lambda+\bar{\Lambda}$ production going across the thresholds is due to charmed baryon production, we estimate a maximum value of $\Delta R \sim 0.35$ as due to this process. A comparison with Table IV shows that this is much smaller than the charmed meson production and explains why it is so difficult to detect charmed baryons in individual channels. Furthermore, the Λ and $\bar{\Lambda}$ increase is smaller than the $p+\bar{p}$ increase, which indicates that Λ, Σ^0, and therefore $\Sigma^\pm$ production is not very large. Most of the increase in R is in $p+\bar{p}$ production; therefore, the most copious decays of Λ_c or Σ_c may be into strange mesons and nucleons.

VIII. HEAVY LEPTON PRODUCTION

We have studied the process[34] $e^+e^- \to \tau^+\tau^-$ by analyzing events of the type

$$e^+e^- \to e^\pm + 1 \text{ prong} + n\gamma \quad (n \geq 0) \qquad (10)$$

where the electron is identified in the LGW. We have confined our analysis to two-prong events because the sequential heavy lepton is expected to decay 85% of the time into a one-charged prong.[35]

Results from this experiment in three energy regions between 4.1 and 7.4 GeV have already been reported.[3] The published data include 60 anomalous electrons, with momentum $p_e \geq 400$ MeV/c, identified in the lead glass wall with a background of 13.9 events. We now have data at the $\psi(3772)$ which we can analyze to investigate the mass of the heavy lepton. The quoted values for this mass from previous analyses are: $M = 1.9 \pm 0.1$ GeV from Perl et al.[36] and $M = 1.91 \pm 0.03$ GeV from PLUTO.[37]

At the ψ'' we have data in the region 3.71 to 3.95 GeV, for an integrated luminosity of 2.18 pb^{-1}. This sample includes ten events with an electron in the LGW[38] and satisfying the same criteria we have used in Ref. 3. The electron identification uses less stringent requirements than those of Section IV.D (i.e., $E_{AC} \geq 150$ MeV and $(E_{AC}+E_{BB}) \geq 0.65$ E). The criteria are:

a) $p_e \geq 400$ MeV/c to achieve good e-π separation in the LGW;

b) $p_{prong} \geq 650$ MeV/c in order to distinguish μ from hadrons in the magnetic detector;

c) the missing mass squared recoiling against the two prongs required to be $MM^2 \geq M_0^2$, an energy dependent cutoff[39] chosen to reduce backgrounds from QED reactions; and

d) coplanarity angle between the two prongs, θ_c, required to be $\geq 20°$, again to reduce QED background.

A. Inclusive Electron Production in Two-Prong Events

First we calculate the inclusive cross section, σ_e, for events of Eq. (10) satisfying our criteria, without any assumptions on heavy lepton production. We use the expression

$$\sigma_e = \frac{N_e}{a_e L}$$

where the acceptance a_e is calculated from the covered solid angle of the two prongs and the efficiencies for triggering the magnetic detector, track reconstruction and other instrumental efficiencies. The results for the ψ" data and the higher energy data are given in Table VII. The background is calculated as explained in Ref. 3; it includes the contribution from events of reaction $e^+e^- \to e^+e^-$, $e^+e^-\gamma$, $e^+e^-e^+e^-$, and from hadronic processes such as $e^+e^- \to hh$.

TABLE VII. Inclusive electron cross sections for two prong events with an anomalous electron with $p_e \geq 400$ MeV/c and other criteria explained in the text.[40]

$E_{c.m.}$	Luminosity (pb^{-1})	Electrons Found	Background Electrons	N_e Corrected	σ_e (nb)	R_e
3.71-3.76	0.22	0	0.7	-1.1 ± 3.5	0.16±0.54	-0.026±0.087
3.76-3.79	1.28	5	2.0	4.5 ± 5.0	0.12±0.13	0.020±0.022
3.79-3.95	0.68	5	1.2	6.8 ± 4.9	0.34±0.25	0.059±0.042
4.1 - 4.2	1.03	8	2.1	8.7 ± 6.4	0.29±0.22	0.058±0.042
4.4 - 5.8	2.71	19	4.1	23.5 ± 9.9	0.29±0.12	0.081±0.034
6.4 - 7.4	5.52	33	7.8	37 ± 13	0.23±0.08	0.126±0.043

Figure 17(a) shows R_e versus $E_{c.m.}$ The point at 3.774 MeV is one standard deviation above zero, suggesting that the mass of the heavy lepton may be $M_\tau < 1.9$ GeV. Although the statistics are low, we do not observe in the "2-prong electrons" the same dip after the ψ" as for the "multiprong electrons" (see Fig. 12), but we observe a smooth rise of R_e, as expected for τ production.

Second, we assume heavy lepton production and calculate

$$R_\tau = \frac{\sigma_\tau}{\sigma_{\mu\mu}} = \frac{N_e}{2L\, B_e\, A_e\, \sigma_{\mu\mu}}$$

where A_e is now the acceptance including geometrical, kinematical and instrumental efficiencies for the reaction $e^+e^- \to \tau^+\tau^-$. Here one τ is taken to decay into $e\nu_e\nu_\tau$ and the other one into one charged prong plus neutrals, i.e. $\tau \to \mu\nu_\mu\nu_\tau$, $\pi\nu_\tau$, $\rho\nu_\tau$, weighted according to the expected fractions.[35] B_e is the branching fraction of $\tau \to e\nu_e\nu_\tau$ decay for which we have used 18.6%, which is the value obtained in the experiment with the most statistics.[34] For the spectrum calculation we have used V-A and M_τ = 1.85 GeV. This plot is shown in Fig. 17(b), where the point with negative R_τ has not been included. Here the curves have been calculated from the QED cross sections for τ and μ pair productions.

$$R_\tau = \frac{\sigma_\tau}{\sigma_{\mu\mu}} = \frac{1}{\sigma_{\mu\mu}} \cdot \frac{43.4}{s}\, \beta(3-\beta^2) = \frac{\beta(3-\beta^2)}{2}$$

and assuming M_τ = 1.8, 1.85, and 1.9 GeV. The data are in agreement with a mass between 1.8 and 1.9 GeV, although the statistics are not sufficient to pin down the τ mass with good precision.[38]

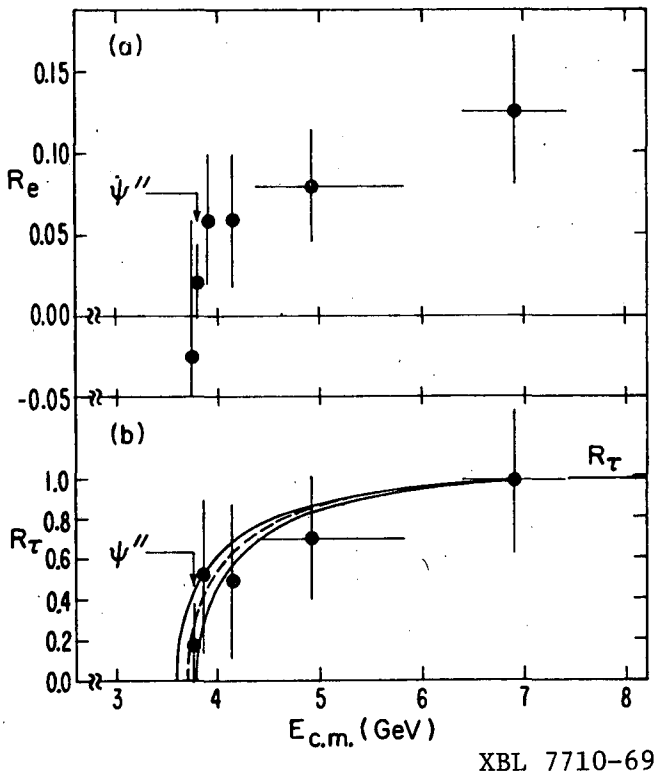

XBL 7710-6971

Fig. 17. Anomalous electron production in 2-prong events with the electron identified in the LGW. (a) Inclusive $R_e = \sigma_e/\sigma_{\mu\mu}$ versus $E_{c.m.}$, (b) $R_\tau = \sigma_\tau/\sigma_{\mu\mu}$, calculated assuming $e^+e^- \to \tau^+\tau^-$ production with subsequent decay of one τ into $e\nu_e\nu_\tau$ and the other one into one-prong only. The arrows indicate the values of the $\psi(3772)$. The curves are calculated assuming the QED point cross sections $R_\tau = 43.4/s \times \beta(3-\beta^2)/2$, where β is v/c for M_τ = 1.8, 1.85, and 1.9 GeV.

B. Background from Charm Production

Next we discuss the background in the electron +1 prong events (Eq. 10) due to semileptonic decays of D mesons that we have measured in the multiprong events. Figure 18 shows the momentum distribution for the 10 electrons and one μ (from one $e\mu$ event) observed at the ψ''. The background from ee and hh events has not been subtracted, but we know that it is larger at the lower momenta, as discussed in Section IV.D. This spectrum should be compared with the one shown in Fig. 10. The two spectra are clearly different; in fact, the two-prong spectrum peaks at $p \sim 800$ MeV/c which

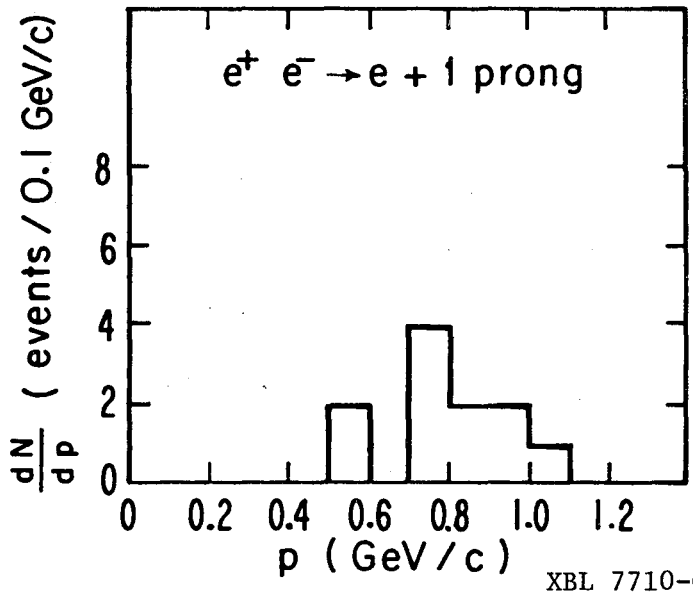

Fig. 18. Momentum distribution for the electrons found in two-prong events in the $\psi(3772)$ energy region. We have included the momentum for the 10 electrons and the μ of the one e-μ event found.

is at a higher value than the peak of the multiprong spectrum (400 MeV/c). The same effect is observed at the higher energies (2-prong spectra not shown here).

In order to calculate the contribution from charm to the two prongs, we need to know (a) the fraction of $D\bar{D}$ pairs producing only one electron and one prong in the final state with total charge $Q = 0$, (b) the fraction of the $D \to e$ spectrum with $p_e \geq 400$ MeV/c, and (c) the fraction of prongs for D decays with $p \geq 650$ MeV/c. The other cuts to be included are the MM^2 and the coplanarity cut. Without these last two factors we estimate, at the ψ'', the background from charm to be $b_c < 13\%$ in the one-prong+electron events (Eq. 10) and $< 3\%$ in the eμ events. At higher energies both R_{charm} (see Table IV) and R_e in two-prongs increase. However, the latter increases by a larger factor than the former so we estimate that the charm background in the two-prongs will not exceed the values quoted for the ψ'' data.

C. Branching Fraction Calculations

The 70 events of Eq. (10) can be studied in more detail in order to measure branching fractions of different τ decay modes. The reactions considered are now:

$$e^+e^- \to \tau^+\tau^- \tag{11a}$$

$$\tau^\pm \to e^\pm \nu_e \nu_\tau \tag{11b}$$

$$\tau^\mp \to \mu^\mp \nu_\mu \nu_\tau \tag{11c}$$

$$\tau^\mp \to h^\mp + \text{neutrals} \tag{11d}$$

The hadron of Eq. (11d) can be a π or a K from $\tau \to \rho\nu_\tau$, $\tau \to \pi\nu_\tau$, $\tau \to K\nu_\tau$, $\tau \to K^*\nu_\tau$, or $\tau \to A_1\nu_\tau$ with A_1 giving only one particle in the detector. From the expected branching fractions[35] we estimate the decay modes contributing to Eq. (11d) to be 45% of the total. Table VIII shows the distribution of events in the various categories. The procedure used to obtain the corrected events from the observed events has been described in Ref. 3. In brief, the background is calculated from the observed ee and hh events and the known

TABLE VIII. Two-prong electron events divided in the different categories. All energies are added together. The background is due to misidentified ee and hh events.

	N (eμ)	N (eμγ)	N (eh)	N (ehγ)
Observed events	22	10	15	23
Background	0.52	1.73	4.12	11.4
Corrected events	21.8 ± 6.3	4.6 ± 5.0	25.5 ± 10.4	28.2 ± 14.1

probabilities of incorrect particle identification; the final corrected events are obtained after background subtraction and corrections (a) for misidentification of h as μ and μ as h, and (b) for detection efficiency. Background from charm has not been subtracted.

In order to calculate branching fractions we write

$$\sigma(e\mu) = 2A_{e\mu}\,\sigma(e^+e^- \to \tau^+\tau^-)\,B_eB_\mu \qquad (12)$$

$$\sigma(eh) = 2A_{eh}\,\sigma(e^+e^- \to \tau^+\tau^-)\,B_eB_h \qquad (13)$$

From the eμ events of Table VIII, the acceptance of the apparatus, the QED τ cross-section, and assuming $B_e = B_\mu$ we can calculate the leptonic branching ratio. Averaging over the different $E_{c.m.}$ energies, including systematic errors, we get (for M_τ = 1.85 GeV)

$$B_e = (20.4 \pm 5.4)\%$$

For the hadronic modes we add the eh and ehγ together, average the acceptance over all the possible modes, use the value of B_e just measured, and obtain, again including systematic errors,

$$B_h = (45 \pm 18)\%$$

in good agreement with the expected[35] value of 45%. In obtaining this value we have not used the 4.6 ± 5.0 eμγ events. These events are not understood at this time, but since the signal is less than one standard deviation we ignore it for the time being.

We have not yet done a separate analysis for the $\tau \to \pi\nu$ and $\tau \to \rho\nu$ decays.[41] Preliminary calculations for the ratio $B(\tau \to \pi\nu)/B(\tau \to \rho\nu)$ yield 0.44 ± 0.37, where we expect 0.5. The errors are large, but the result is not inconsistent with a $\tau \to \pi\nu$ at the expected level.

REFERENCES AND FOOTNOTES

1. The members of the Lead-Glass Wall collaboration are: A. Barbaro-Galtieri, R. Ely, J. M. Feller, A. Fong, P. Lecomte, R. J. Madaras, T. S. Mast, M. T. Ronan, R. R. Ross, B. Sadoulet, T. G. Trippe, V. Vuillemin (Lawrence Berkeley Laboratory and Department of Physics, University of California at Berkeley); J. M. Dorfan, G. J. Feldman, G. Hanson, J. A. Jaros, B. P. Kwan, A. M. Litke, D. Lüke, J. F. Martin, M. L. Perl, I. Peruzzi, M. Piccolo, T. P. Pun, P. A. Rapidis, D. L. Scharre (Stanford Linear Accelerator Center and Department of Physics, Stanford University); B. Gobbi, D. H. Miller (Department of Physics and Astronomy, Northwestern University); S. I. Parker, D. E. Yount (Department of Physics and Astronomy, University of Hawaii).

2. J. E. Augustin et al., Phys. Rev. Letters 34 (1975) 233.

3. A. Barbaro-Galtieri et al., Phys. Rev. Letters 39 (1977) 1058; Lawrence Berkeley Laboratory Report LBL-6458 (1977); and SLAC Report SLAC-PUB-1976.

4. J. M. Feller et al., The Lead-Glass Wall Addition to the SPEAR Mark I Magnetic Detector, Lawrence Berkeley Laboratory Report LBL-6466 (1977), to appear in Proceedings of the IEEE Nuclear Science Symposium, San Francisco, California (1977).

5. P. A. Rapidis et al., Phys. Rev. Letters 39 (1977) 526.

6. J. Siegrist et al., Phys. Rev. Letters 36 (1976) 700.

7. G. Bonneau and F. Martin, Nucl. Phys. B27 (1971) 381; D. R. Yennie, Phys. Rev. Letters 34 (1975) 239; and J. D. Jackson and D. L. Scharre, Nucl. Instr. and Meth. 128 (1975) 13.

8. The formula for this factor can be found in the last paper of Ref. 7.

9. Particle Data Group, "Review of Particle Properties," Rev. Mod. Phys. 48, No. 2, Part II (1976).

10. A. M. Boyarski et al., Phys. Rev. Letters 34 (1975) 1357.

11. V. Lüth et al., Phys. Rev. Letters 35 (1975) 1124.

12. E. Eichten et al., Phys. Rev. Letters 36 (1976) 500; K. Lane and E. Eichten, Phys. Rev. Letters 37 (1976) 477.

13. J. D. Jackson, New Particle Spectroscopy, CERN Report TH.2351 (1977), to appear in Proceedings of the European Conference on Particle Physics, Budapest, Hungary (4-9 July 1977).

14. G. Goldhaber et al., Phys. Letters 69B (1977) 503.

15. P. B. Wilson et al., Stanford Linear Accelerator Report SLAC-PUB-1894 (1977).

16. The systematic uncertainties contributing to the errors are: 0.5 MeV from the long term stability of the E_b monitoring and 0.5 MeV from the absolute momentum calibration.

17. G. Goldhaber et al., Phys. Rev. Letters 37 (1976) 255; I. Peruzzi et al., Phys. Rev. Letters 37 (1976) 569.

18. V. Lüth et al., Stanford Linear Accelerator Report SLAC-PUB-1947 (1977), submitted to Phys. Letters.

19. For more details on the analysis methods used, see I. Peruzzi et al., "Study of D Mesons Produced in the Decay of the $\psi(3772)$," SLAC-PUB-2012 and LBL-6755 (1977), submitted to Phys. Rev. Letters.

20. G. J. Feldman et al., Phys. Rev. Letters 38 (1977) 1313.

21. Many authors have discussed this mass difference. Predictions range from 2 to 15 MeV. For a list of references see Ref. 20 of G. Feldman, "Properties of the D Mesons," SLAC-PUB-2000 (1977), to be published in Proceedings of the 1977 SLAC Summer Institute on Particle Physics, Stanford, California.

22. M. Piccolo et al., SLAC Report SLAC-PUB-1973 and LBL Report LBL-6489 (1977), submitted to Phys. Letters.

23. G. Altarelli, N. Cabibbo, and L. Maiani, Nucl. Phys. B88 (1975) 285; R. L. Kingsley, S. B. Treiman, F. Wilczek, and A. Zee, Phys. Rev. D12 (1975) 2015; M. B. Einhorn and C. Quigg, Phys. Rev. D12 (1975) 2015.

24. D. L. Scharre et al., SLAC Report SLAC-PUB-2019 and LBL Report LBL-6761 (1977), submitted for publication.

25. J. M. Feller et al., Measurement of Semi-leptonic Decays of D Mesons to Electrons at the $\psi(3772)$, Lawrence Berkeley Laboratory Report LBL-6772 (1977), submitted to Phys. Rev. Letters.

26. R. J. Madaras, Anomalous Electron Production in the Lead-Glass Wall Experiment at SPEAR, LBL Report LBL-6766, to be published in Proceedings of the 1977 SLAC Summer Institute on Particle Physics, Stanford, Calif.

27. The electron momentum spectra are derived from the calculations of A. Ali and T. C. Yang, Phys. Letters 65B (1976) 275, and A. Ali, private communication.

28. Measurements done at DORIS on multiprong electron production, at energies $E > 4$ GeV, can be found in W. Braunschweig et al., Phys. Letters 63B (1976) 471; J. Burmester et al., Phys. Letters 64B (1976) 369; R. Brandelik et al., DESY preprint DESY-77/41 (1977).

29. The value of R used in the 6.4 - 7.4 GeV region is from SP-17 data (V. Lüth to be published in Proceedings of the 1977 SLAC Summer Institute on Particle Physics, Stanford, California); the others are from this experiment: Ref. 5 for 3.772 GeV, and unpublished preliminary values for the other two regions.

30. C. Quigg and J. L. Rosner, Hadronic Decays of Charmed Mesons, Fermi National Accelerator Laboratory Report FERMILAB-Pub-77/60-THY (1977).

31. At this writing (October 1977) the SP-26 and SP-17 data on this subject have been combined and a common paper has been submitted for publication: M. Piccolo et al., Inclusive Baryon Production in e^+e^- Annihilation, SLAC-PUB-2023 and LBL-6775 (1977).

32. A. De Rujula, H. Georgi and S. L. Glashow, Phys. Rev. D12 (1975) 147.

33. E. G. Cazzoli et al., Phys. Rev. Letters 34 (1975) 1125; and B. Knapp et al., Phys. Rev. Letters 37 (1976) 882.

34. First reported by M. L. Perl et al., Phys. Rev. Letters 35 (1975) 1489, and Phys. Letters 63B (1976) 466. For a recent review on this subject, see M. Perl, Proceedings of the XII Rencontre de Moriond, edited by Trân Thanh Van, RMIEM, Orsay (to be published), also issued as SLAC-PUB-1923 (April 1977). See also M. L. Perl, these Proceedings.

35. H. B. Tacker and J. J. Sakurai, Phys. Letters 36B (1971) 103. Also Y. S. Tsai, Phys. Rev. D4 (1971) 2821. For updated predictions, see G. J. Feldman in Proceedings of the 1976 Summer Institute on Particle Physics (SLAC 1976), also issued as SLAC-PUB-1852 (1976).

36. M. L. Perl et al., Properties of the Proposed τ Charged Lepton, SLAC Report SLAC-PUB-1997 and LBL Report LBL-6731 (1977). Submitted to Phys. Letters.

37. G. Flügge, Review of Heavy Leptons in e^+e^- Annihilation, DESY Report DESY-77/35 (1977), to appear in Proceedings of the Vth International Conference on Experimental Meson Spectroscopy, Northeastern University, Boston, Massachusetts (1977).

38. The analysis of these data, using only the magnetic detector information, can be found in the paper of M. Perl, Review of Heavy Lepton Data, in these Proceedings.

39. $M_o^2 = 0.8$ GeV^2 for $E_{c.m.} \leq 4.4$ GeV, $M_o^2 = 1.1$ GeV^2 for $4.4 < E_{c.m.} \leq 6.0$ GeV, and $M_o^2 = 1.5$ GeV^2 for $E_{c.m.} > 6$ GeV.

40. For the energies above 4 GeV we have increased the luminosity by a factor of 1.08, which was missing in Ref. 3. This factor has the effect of reducing the branching ratios of Ref. 3 by 4%. All the luminosities quoted in this talk have been corrected by the 1.08 factor.

41. The DASP group has reported at this conference a measurement for $B(\tau \to \rho\nu_\tau)$; they also report that their signal for $\tau \to \pi\nu_\tau$ is smaller than expected. See the presentation by S. Yamada in these Proceedings.

TECHNICAL INFORMATION DEPARTMENT
LAWRENCE BERKELEY LABORATORY
UNIVERSITY OF CALIFORNIA
BERKELEY, CALIFORNIA 94720